Stuck in a State of Inattention? Functional Hyperconnectivity as an Indicator of Disturbed Intrinsic Brain Dynamics in Adolescents With Concussion: A Pilot Study

Angela M. Muller[1] and Naznin Virji-Babul[1]

Abstract

Sports-related concussion in youth is a major public health issue. Evaluating the diffuse and often subtle changes in structure and function that occur in the brain, particularly in this population, remains a significant challenge. The goal of this pilot study was to evaluate the relationship between the intrinsic dynamics of the brain using resting-state functional magnetic resonance imaging (rs-fMRI) and relate these findings to structural brain correlates from diffusion tensor imaging in a group of adolescents with sports-related concussions ($n = 6$) and a group of healthy adolescent athletes ($n = 6$). We analyzed rs-fMRI data using a sliding windows approach and related the functional findings to structural brain correlates by applying graph theory analysis to the diffusion tensor imaging data. Within the resting-state condition, we extracted three separate brain states in both groups. Our analysis revealed that the brain dynamics in healthy adolescents was characterized by a dynamic pattern, shifting equally between three brain states; however, in adolescents with concussion, the pattern was more static with a longer time spent in one brain state. Importantly, this lack of dynamic flexibility in the concussed group was associated with increased nodal strength in the left middle frontal gyrus, suggesting reorganization in a region related to attention. This preliminary report shows that both the intrinsic brain dynamics and structural organization are altered in networks related to attention in adolescents with concussion. This first report in adolescents will be used to inform future studies in a larger cohort.

Introduction

Approximately 42 million people worldwide are diagnosed with concussion (also referred to as mild traumatic brain injury [mTBI]) every year (Gardner and Yaffe, 2015). The typical consequences of concussion are deficits in working memory, executive function, and attention in addition to symptoms such as headaches, dizziness, fatigue, and sleep disturbances. Most adults who sustain a single concussion recover fully within days; however, children and adolescents take longer to recover and may be more vulnerable to the effects of a sports-related concussion (Anderson et al., 2009; Barlow et al., 2010).

A major challenge in understanding the effects of concussion stems from gaps in knowledge about the relationship between symptoms, cognitive function, and the evolving changes in the brain. Conventional clinical neuroimaging tools (such as computed tomography and magnetic resonance imaging [MRI]) cannot detect the widespread and often subtle changes in structure and

[1]Department of Physical Therapy, Faculty of Medicine, University of British Columbia, Vancouver, BC, Canada

Corresponding Author:
Angela M. Muller, Djavad Mowafaghian Centre for Brain Health, University of British Columbia, 2215 Wesbrook Mall, Vancouver, BC V6T 1Z3, Canada.
Email: angelamartinamueller@outlook.com

function that occur in the brain following concussion. In addition, the diffuse and continually evolving secondary changes that are the hallmark of concussion require tools that can dynamically probe the changing state of the brain. Diffusion tensor imaging (DTI), which detects changes in the white matter microsturecture, shows that the stretching and tearing of the brain tissue caused by the acceleration and deceleration forces acting upon the head during impact results in a diffuse disconnection pattern affecting the entire white matter architecture of the brain (Hellyer et al., 2013; Caeyenberghs et al., 2014; Iraji et al., 2016; Hayes et al., 2017).

Structural alterations, no matter how subtle and diffuse, are invariably associated with changes in physiology and altered brain function. Resting-state functional magnetic resonance imaging (rs-fMRI) investigating the intrinsic fluctuations of the blood oxygen-level dependent (BOLD) signal is particularly sensitive to changes in brain function following concussion. These studies show that concussion changes the intrinsic connectivity networks (ICNs) of the brain and alters the functional connection strength between different brain regions. In particular, the default mode network (DMN) and the salience network frequently show impaired inter and intranetwork activity following a brain injury (Bonelle et al., 2011; Mayer et al., 2011; Bonelle et al., 2012; Sours et al., 2013; Hillary et al., 2014; Sharp et al., 2014; Sours et al., 2015). A prominent feature of concussion is a diffuse increase in functional connectivity or *hyperconnectivity* (Johnson et al., 2012; Borich et al., 2015; Czerniak et al., 2015; Caeyenberghs et al., 2017; Militana et al., 2016; Newsome et al., 2016; Churchill et al., 2017).

Hyperconnectivity represents a deviation from the healthy state and is usually interpreted as maladaptive plasticity resulting from the brain injury (Johnson et al., 2012; Newsome et al., 2016; Churchill et al., 2017), particularly when associated with impaired cognition. Hyperconnectivity has also been observed with preserved or recovered cognitive performance and may represent positive functional plasticity as a compensation for persistent structural alterations (Shumskaya et al., 2012; Bharat et al., 2015; Burianová et al., 2015; Czerniak et al., 2015; Marstaller et al., 2015; Olsen et al., 2015; Agarwal et al., 2016; Harris et al., 2016; Iraji et al., 2016); however, little is known about the nature of the underlying processes of this pattern or its functional significance.

Hillary et al. (2014) suggest that brain regions demonstrating functional hyperconnectivity as a consequence of concussion almost always belong to a group of brain regions forming the so-called rich club. The *rich club* of the brain is constituted of a specific group of brain regions that are all highly interconnected with themselves and build the structural white matter backbone of the brain (van den Heuvel and Sporns, 2011). In addition,

recent DTI studies (Gollo et al., 2015; Betzel et al., 2016) show that these rich club regions are particularly involved in driving the intrinsic brain dynamics. Due to these relationships between hyperconnectivity and rich club nodes, and between rich club nodes and intrinsic brain dynamics, we felt it was important to gain a better understanding of which underlying structural changes are associated with hyperconnectivity in the concussed brain and how these structural changes might affect the intrinsic brain dynamics.

We have previously reported on the changes in rs-fMRI and diffusion MRI data in a group of adolescent athletes with concussion and healthy matched controls. Our rs-fMRI analysis revealed altered intraconnectivity in the DMN and increased connectivity strength or hyperconnectivity in two frontal regions (Borich et al., 2015); analyses of the DTI data revealed a whole brain increase in fractional anisotropy (FA) and a decrease in mean diffusivity (MD) in the concussion group compared with the healthy controls (Virji-Babul et al., 2013). In particular, we found increased FA in frontal tracts, predominantly in the anterior corona radiata in the concussed group (Borich et al., 2013). In this previous work, we evaluated the changes in brain structure and function *separately*. We felt it was important to now investigate the relationship between brain function and the associated structural correlates.

The vast majority of studies using rs-fMRI (including our own) implicitly assume temporal stationarity of the ICNs. However, this assumption is an oversimplification. ICNs are not stationary but are dynamic and switch between different brain states within a single scanning session. The strength as well as the directionality of the connections between brain regions vary over short time scales from seconds to minutes, and brain regions might belong to different ICNs at different time points (Chang and Glover, 2010; Jones et al., 2012; Hutchison et al., 2013). When shorter time windows are analyzed, even the DMN and the dorsal attention network that are characterized by strong anticorrelations when their time courses are averaged over the entire length of the data acquisition show periods of synchronized activity (Chang and Glover, 2010).

The aim of this pilot study was to investigate how concussion alters the temporal dynamics of resting-state networks and how these alterations are associated with the alterations in the structural organization of the brain. Specifically, we hypothesize (a) that hyperconnectivity or the prolonged synchronization of parts of the intrinsic network architecture will be evident as a disruption of the highly dynamical interplay between the different ICNs in adolescents with concussion compared with healthy controls and (b) that the disrupted intrinsic brain dynamic will be associated with the structural integrity of the rich club brain regions.

Table 1. Demographics of the Participants.

ID	Sex	Age	Total score on SCAT2	Number of concussions	Days after injury
Con_001	M	14	90	1	30
Con_002	F	17	79	3	17
Con_006	M	17	76	2	24
Con_008	M	15	86	1	30
Con_009	M	15	92	3	30
Con_011	M	16	89	2	31
	5 M/1F	$M = 15.67$	$M = 85.33$	$M = 2$	$M = 27$
HC_001	F	16	85	–	–
HC_002	M	14	96	–	–
HC_003	M	16	93	–	–
HC_005	M	17	92	–	–
HC_006	M	16	88	–	–
HC_008	M	16	87	–	–
	5 M/1F	$M = 15.83$	$M = 90.17$	–	
Statistics		$X^2 = 0.0635; p < .881$	$X^2 = 1.4474; p < .229$		

Note: SCAT2 = Sport Concussion Assessment Tool 2. Version.

Methods

Participants

We reanalyzed the structural and task-free fMRI data of six adolescent athletes (mean age = 15.5 years) with a clinical diagnosis of subacute concussion (≤2 months prior) and six healthy adolescents matched for age, level of physical activity, and motion during MRI acquisition. The study sample is part of a larger data set that was acquired in our laboratory from 2011 to 2012. We excluded 10 participants from the original sample due to rigorous control for motion. Table 1 provides demographic information about all participants. Additional information can be found in Virji-Babul et al. (2013) and Borich et al. (2015). The adolescents' parents gave written informed consent for their children's participation under the approval of the ethics committee of the University of British Columbia and in accordance with the Helsinki declaration.

Data

The MRI data were collected at the University of British Columbia's 3 T Research Facility on a Philips Achieva 3.0 T MRI scanner (Philips Healthcare, Andover, MD) using an eight-channel sensitivity encoding head coil (SENSE factor 2.4) and parallel imaging. The following images were acquired: (a) A T1 weighted TFE-SENSE sequence with repetition time (TR) = 8 ms, echo time (TE) = 3.7 ms, flip angle $\theta = 6°$, field of view (FOV) $256 \times 256 \times 160 \, \text{mm}^3$, isotropic voxel size = $1 \times 1 \times 1 \, \text{mm}^3$, 160 slices per volume, acquisition duration 335 s. (b) A whole-brain high-angular imaging resolution diffusion imaging sequence with two diffusion-weighted scans performed with a single-shot echoplanar imaging sequence of TR = 7013 ms, TE = 60 ms, FOV = $224 \times 224 \, \text{mm}$, 70 slices, isotropic voxels $2.2 \times 2.2 \times 2.2 \, \text{mm}^3$, time of acquisition = 7 min. Diffusion weighting was performed across 60 different noncollinear orientations ($b = 700 \, \text{s/mm}^2$). Ten minimally weighted ($b = 0$) diffusion images were also acquired. (c) A task-free BOLD signals single shot whole-brain echoplanar imaging sequence with a TR = 2000 ms, TE = 30 ms, flip angle = $\theta = 90°$, FOV = $240 \times 143 \times 240 \, \text{mm}^3$, isotropic voxels $3 \times 3 \times 3 \, \text{mm}^3$ ascending acquisition with $1 \, \text{mm}^3$ gap, 36 slices per volume, acquisition time 8.2 min, 240 volumes. Participants were instructed to relax and to lie as motionless as possible while keeping the eyes fixed on a target and thinking of nothing in particular.

Preprocessing of the Functional Data

All preprocessing steps of the fMRI data are listed in the following and were performed using the SPM12 software (http://www.fil.ion.ucl.ac.uk/spm) running on MATLAB (MATLAB R2016a, The Math Works Inc.). Figure 1 shows a visual representation of the processing and analysis steps for the fMRI data.

First, the first 10 volumes of the task-free fMRI data were discarded allowing for T1 saturation effects, leaving 230 volumes for the analysis and then realigned in a two-pass procedure to correct for potential head movements during the task-free scan. Second, the fMRI time series were slice time corrected for the ascending acquisition. Third, the T1 weighted anatomical image was coregistered
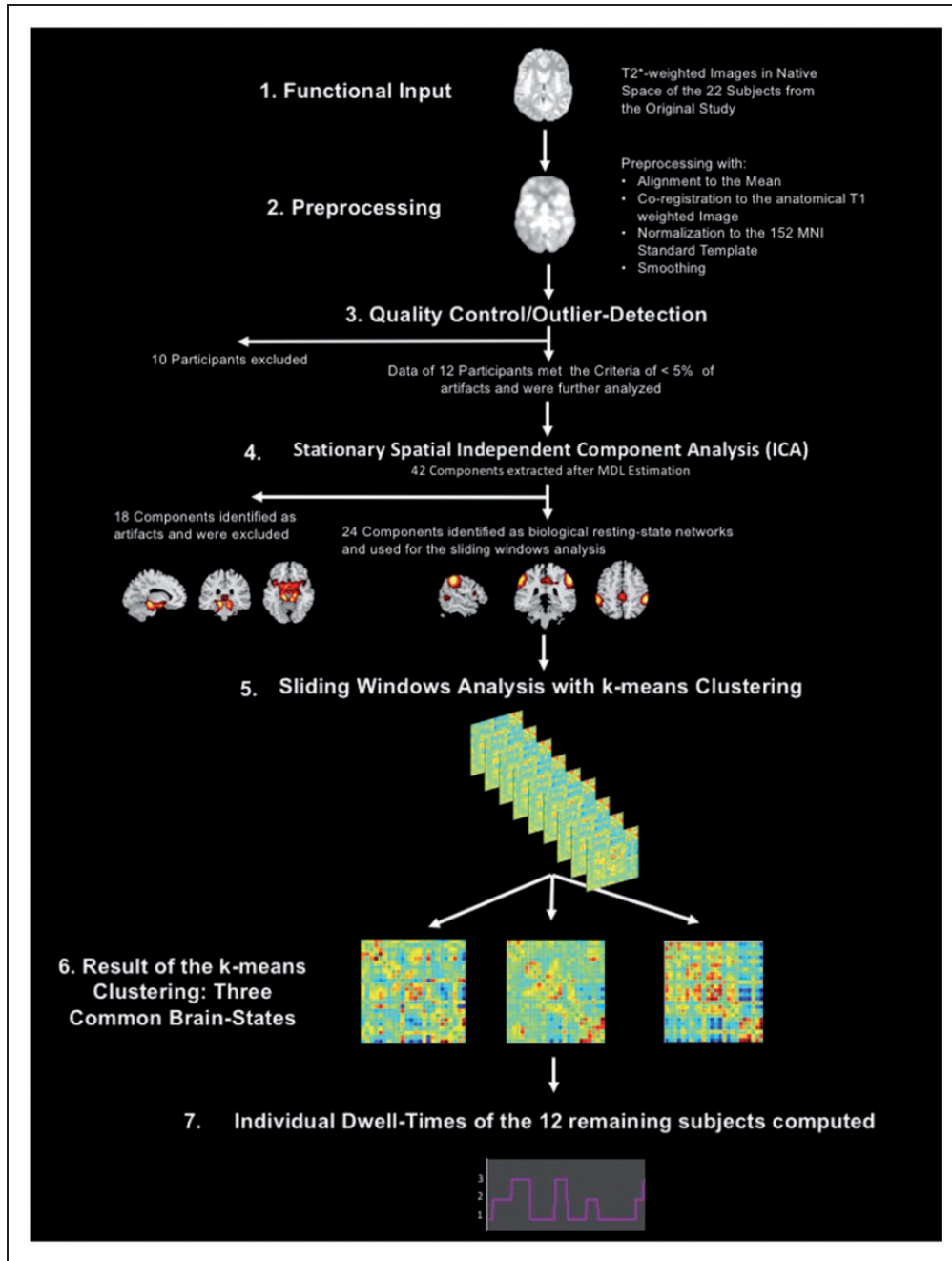
Figure 1. Visual representation of the processing and analysis steps for the fMRI data.
fMRI = functional magnetic resonance imaging.

to the mean functional image generated during the alignment step. Fourth, the T1 weighted anatomical images were segmented into the three tissue classes, gray matter (GM), white matter (WM), and cerebrospinal fluid (CSF) in native space. Fifth, a study population-specific GM template was generated using the Diffeomorphic Anatomical Registration using Exponentiated Lie algebra (DARTEL) procedure routine (Ashburner, 2007) implemented in SPM12 that allows for a high-dimensional and nonlinear registration of the anatomical and functional images and

their subsequent normalization to the Montréal Neurological Institute (MNI) template. The functional and the anatomical data subsequently used for the functional analyses were resampled to a 2-mm isotropic voxel size during this step. In the final step, the functional images were smoothed using an isotropic Gaussian kernel full width at half maximum (FWHM 6 mm). To assess the effect of motion on the quality of the functional data, we controlled the output for the three translational and the three rotational motion parameters to make sure that

none of the six parameters surpassed a displacement >1 mm (following the approach of Power et al., 2012, the rotational displacements were calculated at a 50 mm radius). In addition, we performed an outlier detection using the Artifact Detection Toolbox (ART) (http://www.nitrc.org/projects/artifact_detect/) as implemented in the preprocessing pipeline of Conn Version 17 a (scan-to-scan global signal z value threshold = 3; scan-to-scan composite motion threshold = 0.5 mm). Because the results of dynamical intrinsic connectivity analyses are much more susceptible to head motion in comparison with static connectivity analyses (Laumann et al., 2017), we used a very rigorous threshold to control for motion artifacts. Only participants who showed less than 5% outliers over the 230 analyzed functional volumes were selected for this pilot study (average number of outlier volumes over all included participants = 5.91; $SD = 3.17$; Max = 11; Min = 2). In a final step, we tested for potential significant differences in number of outliers between the adolescents with concussion and the healthy controls using a two-sample t test. The two-sided t test revealed no significant differences in outliers between the concussed and the healthy group, $t(10) = .026$; $p = .799$.

Computation of a Stationary Spatial Independent Component Analysis

For the independent component analysis (ICA), we used the MATLAB-based Group ICA of the fMRI Toolbox (GIFT) v4.0 a (http://mialab.mrn.org/software/gift/). ICA is a statistical method of blind signal source separation. Assuming a generative model and a linear mixture of independent sources, it works with higher order statistics to maximize the spatial or temporal independence of the data and to identify the independent components hidden in the signal (Calhoun et al., 2001). The Minimum Description Length (MDL) criteria were applied to estimate the number of independent components in our data (mean MDL over all subjects = 41.75; $SD = 4.02$). Next, a subject-specific Principal Component Analysis (PCA) using the expectation maximization algorithm was computed retaining 63 components for data reduction on subject level, and then an ICA using the Infomax algorithm (repeated 100 times in ICASSO (Himberg et al., 2004) using random initial conditions to improve the stability of the final decomposition) was computed to extract 42 components on study sample level. To map the sample spatial maps back into the subject space and to compute the subject-specific time courses, the GICA1 algorithm was applied that uses the projection matrices generated by combining the group-level unmixing matrix created during the ICA with the subject-level matrices derived during the PCA (Calhoun et al., 2001; Cole et al., 2010). For visual inspection and classification, the group spatial maps were thresholded at $z = 2$. The 42 components were then evaluated using the following criteria: location of the

component's peak voxel in gray matter; highest power accumulated on the left side of the component time-course power spectrum, that is, <0.01 Hz; no activations in the ventricles or white matter or near and following blood vessels; no motion artifacts (activity pattern resembling a halo around the brain). Twenty-four of the 42 extracted components were identified as neurobiologically meaningful, that is, representing ICNs known from the literature, and used for the subsequent sliding window analysis (SWA).

Dynamical Intrinsic Connectivity Analysis Using a Sliding Windows Approach on Network Level

The time courses were preprocessed by detrending (linear, quadratic, and cubic trends) and despiking (for the removal of potential residual motion artifacts, which are not wholly removed by the linear regression of the six motion parameters; Power et al., 2012). The time points identified as outliers by ART were not censored but effectively removed by dummy coding them during the regression of the motion parameters. This approach has the advantage that the continuity of the time series is still preserved, which is an important assumption for the subsequent low-pass filtering with a high-frequency cutoff of 0.15 Hz and also for the SWA explained in the following section.

For the SWA, we used the following parameters: tapered windows (Gaussian $\sigma = 3$ TR) of 30 volumes (=60 s) were moved forward in 1 TR steps resulting in 200 windows for each participant. A k-means cluster analysis using the L1 distance function was applied to identify the recurring patterns of intrinsic connectivity (or brain states) between the 24 components identified as representing meaningful ICN. The number of clusters to extract from the data was previously estimated by using the silhouette algorithm (Rousseeuw, 1987). The silhouette coefficient measures how similar an object is to its own cluster compared with all the others clusters, when all objects have a high silhouette value, the clustering configuration is a good fit for the underlying data structure. The silhouette algorithm revealed three common brain states over all participants as an appropriate fit.

We used a t test to test for significant groupwise differences of the time that each group spent in each of the three brain states during the functional scan.

Preprocessing of the DTI Data

The ExploreDTI toolbox (Leemans et al., 2009) was used to preprocess and analyze the DTI data. Figure 2 shows a visual representation of the processing and analysis steps for the DTI data.

First, the raw data were converted to NIFTI files using the dcm2nii tool included in the MRIcron toolbox. Second, the data of each participant were loaded into ExploreDTI and visually inspected for quality control.
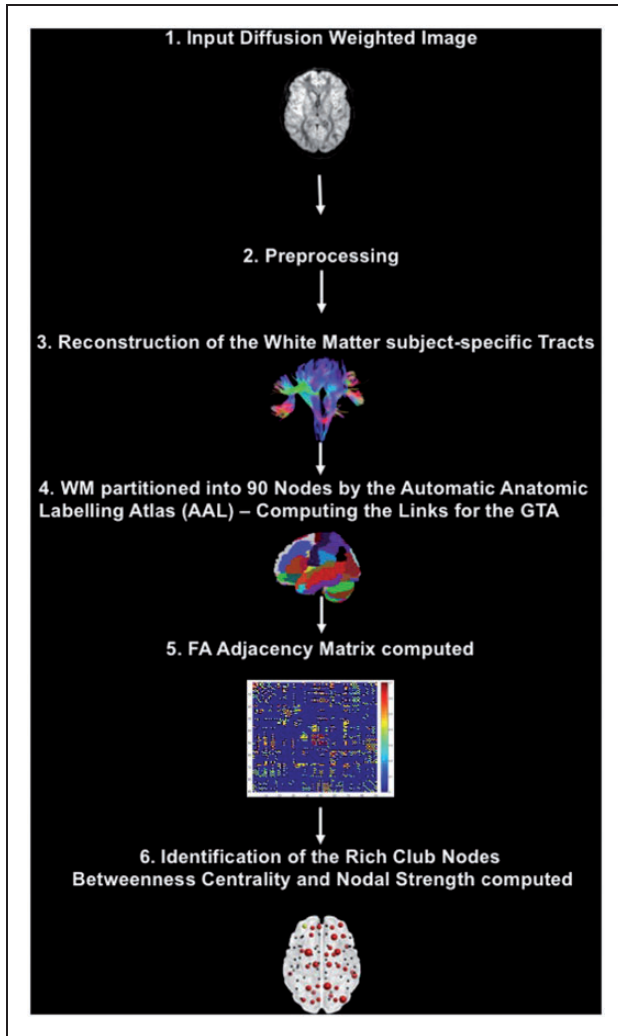
Figure 2. Visual representation of the processing and analysis steps for the DTI data.
GTA = graph theoretical analysis; DTI = diffusion tensor imaging; FA = fractional anisotropy.

Next, the data were corrected for subject motion and eddy current-induced geometric distortions (Leemans and Jones, 2009). Tensor estimation was applied using the robust estimation of tensors by outlier rejection approach (Chang et al., 2005). For the reconstruction of the WM subject-specific tracts, starting seed points were uniformly placed through the data at 2 mm resolution. The trajectory propagation was terminated as soon as the FA values decreased below a cutoff threshold of <0.2 or the angle between two consecutive steps was higher than 45 degrees.

Graph Theoretical Analysis of the White Matter Architecture

Graph theoretical analysis (GTA) is a mathematical branch that analyses and describes complex network structures like the brain using two basic elements: nodes (or vertices) and links (or edges) connecting the nodes of the network. GTA measures account for different qualities of these two elements and characterizes and quantifies a large number of network-specific features on whole network level as well as on single-node level. This type of analysis provides key information about how a specific network architecture might be more efficient than other configurations or how the change in a single node may affect the entire whole network structure.

The first step of every GTA is to define the nodes and the links. We used 90 macroanatomical regions as defined by the Automatic Anatomic Labelling Atlas (AAL; Tzourio-Mazoyer et al., 2002) to structurally parcellate the brain into nodes, and the FA values of the white matter tracts connections between these 90 regions to define the links.

Defining the Rich Club Members and Node Selection for Further GTAs

Previous studies (Gollo et al., 2015; Betzel et al., 2016; Deco et al., 2016) have shown that a specific subgroup of nodes, the so-called rich club nodes, are particularly vital for the intrinsic functional dynamics of the brain. The term *rich club* describes brain regions that are proper connector hubs, that is, nodes that are characterized by a high *degree* (k) of connections in relation to other nodes but also play a central role in the regulation of the information flow because they are mainly interconnected with other connector hubs displaying the same qualities as themselves (van den Heuvel and Sporns, 2011). For this reason, we identified the *rich club* nodes in the white matter architecture of the healthy controls by computing the *rich club distribution* using the algorithm for weighted rich clubs from the BCT toolbox (Rubinov and Sporns, 2010). Because random networks can also exhibit *rich club* formations by chance, an important step for the identification of the rich club nodes in the human brain is the standardization of the empirical *rich club distribution* by the rich club distribution computed for equivalent random networks. Only nodes whose *rich club coefficients* surpass a threshold of 1 after the standardization process qualify as biologically meaningful *rich club* nodes. For this purpose, we generated 500 random networks that preserved the original distribution of the weighted connections or *nodal strength* of the empirical network using the randomization algorithm with 30 iterations from the BCT toolbox (Rubinov and Sporns, 2010) and then computed the rich club distribution for these 500 random networks. As a final step, after identifying the *rich club* nodes in the healthy controls, we computed the *rich club distribution* for the adolescents with concussion and used a one-sided nonparametric Wilcoxon–Mann test to determine k levels for which the *rich club coefficient* of the

healthy controls was significantly higher than the *rich club coefficient* of the concussed athletes.

To minimize the number of necessary corrections for multiple comparisons, only the 36 nodes of the healthy controls were chosen for the subsequent GTA analyses. To be selected for the final GTA, these 36 nodes had to be qualified as biologically meaningful *rich club* members by displaying a *standardized rich club coefficient* higher than 1, and their *k* levels were also in the *k* level range where the *rich club coefficient* of the two groups had shown significant differences.

Selection of the GTA Measures

We used the algorithms in the BCT toolbox (Rubinov and Sporns, 2010) to compute the GTA measures of *nodal strength* and *betweenness centrality* for the 36 *rich club* members. *Nodal strength* is the sum of all weighted positive connections of a node (Rubinov and Sporns, 2011) and takes into account the strength of the connections. *Betweenness centrality* characterizes a node's importance for an effective information flow. A high value in *betweenness centrality* indicates that it is an important connector hub. *Betweenness centrality* quantifies a node's/region's number of the shortest path lengths that cross that region. Shortness of path length is not defined by the actual anatomical distance between two brain regions/nodes but by the minimal number of nodes that must be passed to connect region/node A with region/node B. Short path lengths are associated with decreased wiring cost, energy consumption, and time delay.

Modeling the Relationship of the Intrinsic Functional Brain Dynamics and White Matter Architecture

When evaluating the intrinsic functional brain dynamics, it is critical to evaluate the length of time spent in each brain state. This is referred to as dwell time. A brain that smoothly switches between the different brain states such that equal time is spent in each of the brain states has a different dynamic profile than a brain that remains in one of the brain states for a prolonged time frame. We calculated the number of 60-s windows in each of the three brain states. We then correlated these numbers with the *betweenness centrality* and *nodal strength* values of the subjects' 36 rich club nodes using Spearman correlation as none of the variables displayed a normal distribution.

Results

Spatial Stationary ICA

From the 42 components that were extracted by the ICA, 24 components were identified to represent biologically meaningful ICNs (Table 2; Figure 3).

Sliding Windows Analysis

We computed 200 windows of 30 TRs = 60 s length for each of the 12 participants, that is, overall 2,400 windows, and extracted three common brain states using *k*-mean clustering.

Brain State 1 (Figure 4(a)) occurred 634 times or during 26% of the analyzed 2,400 windows. Its network constellation is characterized by a coupling or positive correlation between the five visual networks (PrimVis, HighVis, Ling, inferior occipital gyrus, and Precun), by a positive coupling of four networks representing a functional interface between primary in- and output functions (vision, hearing, motion, and visceral sensation) and attention (pIns, supplementary motor area, dorsal attention network, and frontoparietal network) and a positive coupling of three higher order networks (Lang, left

Table 2. Identification of the Elected Components.

| Component	Identification	Component	Identification
C02	Bilateral rolandic operculum network (RolOp)	C21	Anterior DMN (aDMN)
C03	Posterior DMN (pDMN)	C23	Higher visual network (HighVis)
C04	Bilateral paracentral network (Paracent)	C24	Left executive-control network (LECN)
C05	Language network (Lang)	C25	Precuneus network (Precun)
C06	Primary visual network (PrimVis)	C26	Bilateral inferior frontal gyrus network (bilIFG
C07	Anterior cingulate network (ACC)	C28	Dorsal attention network (DAN)
C08	Bilateral supplementary motor area (SMA)	C29	Frontoparietal network (FPN)
C09	Bilateral auditory network (Aud)	C30	Bilateral posterior middle temporal gyrus network (pMTG)
C11	Bilateral sensorimotor network (SM)	C31	Right pars triangularis network (rTriang)
C12	Right executive-control network (RECN)	C32	Bilateral middle frontal gyrus network (bilMFG)
C17	Bilateral posterior insula network (pIns)	C38	Bilateral inferior occipital gyrus network (IOG)
C20	Bilateral fusiform gyrus network (Fus)	C39	Bilateral lingual gyrus network (Ling)

Note. DMN = default mode network.
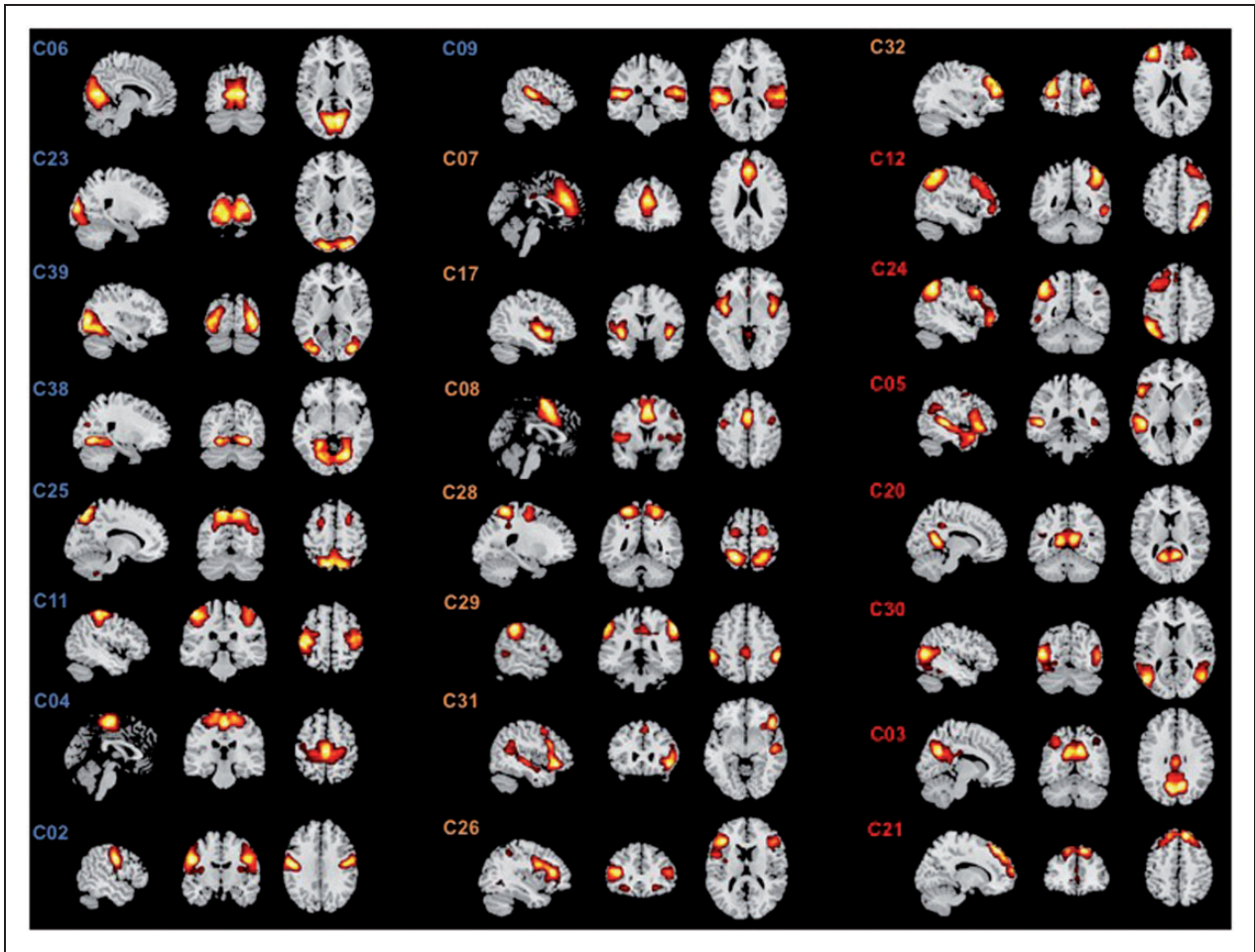
Figure 3. The 24 ICA components selected for the SWA. Figure 3 shows the 24 ICA components that were used for the subsequent SWA grouped by their subsystem membership. The ICs forming the primary-perception-production subsystem are highlighted by blue-colored labels in the figure: C06 = primary visual network (PrimVis); C23 = higher visual network (HighVis); C39 = bilateral lingual gyrus network (Ling); C38 = bilateral inferior occipital gyrus network (IOG); C25 = precuneus network (Precun); C11 = bilateral sensorimotor network (SM); C04 = bilateral paracentral network (Paracent); C02 = bilateral rolandic operculum network (RolOp); C09 = bilateral auditory network (Aud). The ICs forming the In-Output-Attention interface are highlighted by orange-colored labels in the figure: C07 = anterior cingulate network (ACC); C17 = bilateral posterior insula (pIns) network; C08 = bilateral supplementary motor area (SMA); C28 = dorsal attention network (DAN); C29 = frontoparietal network (FPN); C31 = right pars triangularis network (rTriang); C26 = bilateral inferior frontal gyrus network (bilIFG); C32 = bilateral middle frontal gyrus network (bilMFG). The ICs constituting the higher cognition functions subsystem are highlighted by recolored labels in the figure: C12 = right executive-control network (RECN); C24 = left executive-control network (LECN); C05 = language network (Lang); C20 = bilateral fusiform gyrus network (Fus); C30 = bilateral posterior middle temporal gyrus network (pMTG); C03 = posterior DMN (pDMN); C21 = anterior DMN (aDMN). SWA = sliding windows analysis; ICA = independent component analysis; ICs = independent components.

executive-control network [LECN], posterior DMN) with the anterior DMN. There is a decoupling or negative correlation between the networks representing the in-output-attention interface and the higher order networks represented by LECN, Lang, Fus, aDMN, and pDMN.

Brain State 2 (Figure 4(b)) was the most frequent state with 1,100 occurrences or during 46% of the total windows. It is characterized by a positive coupling of the five visual networks and by a positive coupling of the motor networks (RolOp, SM, and Paracent) with each other and with the auditory network. The auditory network

shows also a positive coupling with the networks representing the in-output-attention interface whose constituent networks also show a higher positive coupling with each other than with the other networks. The higher order networks LECN, Fusi, Lang, aDMN, and pDMN are likewise coupled with each other and form a separate subconfiguration that is segregated from the in-output-attention interface by anticorrelations.

Brain State 3 (Figure 4(c)) occurred 656 times or in 27% of the analyzed 2,400 windows. This brain state displays a network constellation that is characterized by a
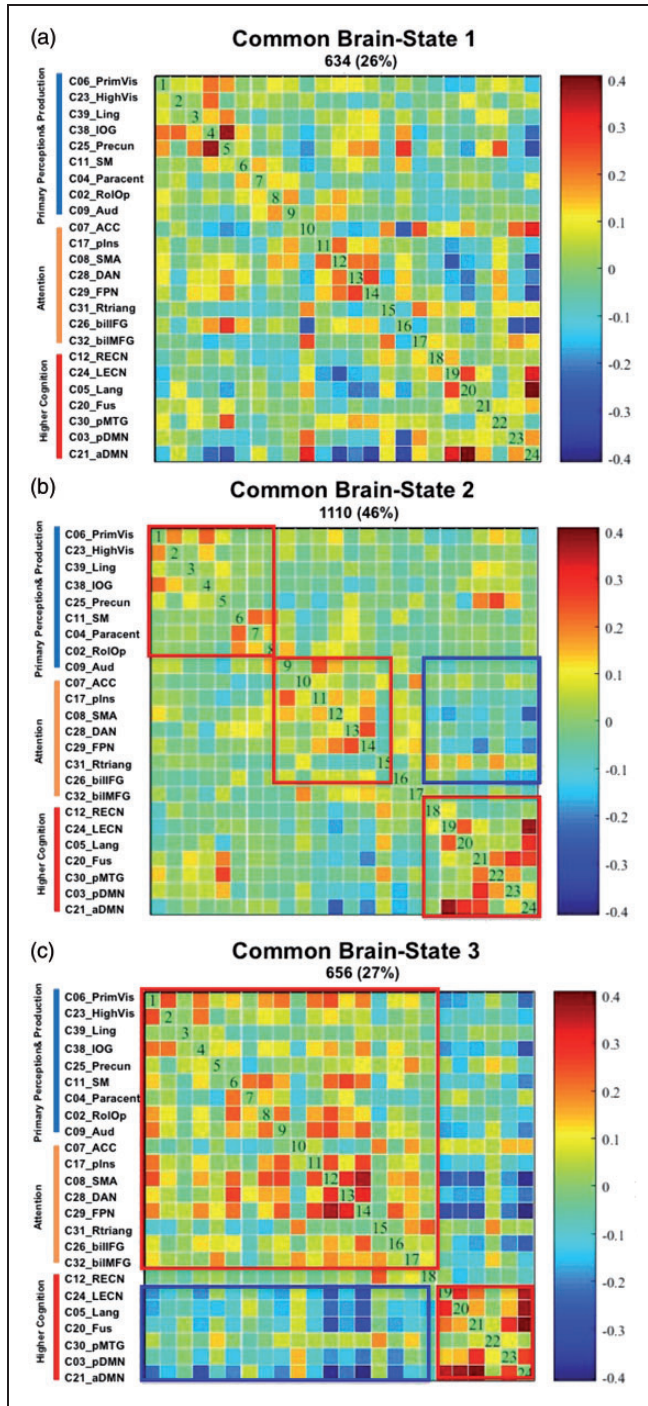
Figure 4. The three brain states. (a–c) The different network configurations of the three brain states that were extracted using *k*-mean clustering of the 2,400 windows (200 windows of 30 TRs = 60s length for each of the 12 participants) that were analyzed in the context of the SWA. The cluster matrixes show the 24 ICs arranged in three groups; group membership is indicated by colored bars on the left side (blue = ICs representing primary perception [auditory and visual] and production [motion] networks, orange = ICs representing attention networks, and red representing higher order cognitive network). Red rectangles highlight positive correlations or coupling between networks/ICs,

(continued)

coupling of the visual, motor, and auditory networks with the networks representing the in-output-attention interface. In addition, it shows a clear decoupling from the higher order networks represented by right executive-control network, LECN, Lang, aDMN, and pDMN, which show a strong positive coupling with each other.

A subsequent *t* test aimed to elucidate potential group-specific differences of the intrinsic functional brain dynamics in patients and healthy controls. While the healthy controls spent approximately the same time in each of the three brain states (between 35 and 45 windows), the concussed group spent most of the time in Brain State 2 (about 65 windows) and clearly less time (around 20 windows) in the Brain States 1 and 3. The *t* test revealed groupwise significant differences between the dwell times for Brain States 2 and 3. The concussed group spent significantly more time in Brain State 2 ($t = 2.62$; $p = .0254$) than the healthy controls, and the latter spent significantly more time in Brain State 3 ($t = 2.532$; $p = .0302$) than the concussed group (Figure 5).

GTA Analysis of the White Matter Architecture

Using the criteria described in the Methods section (see Figure 6 for illustration and Table 3 for the statistics), we identified 36 nodes as representing the *rich club* nodes in the healthy controls (Figure 7(a) and Table 4). The individual dwell times of the brain states were correlated with the corresponding values of *nodal strength* and *betweenness connectivity*. Thirteen nodes showed a significant correlation before correction for multiple comparisons (Table 4); however, only one association of individual dwelling time in Brain State 3 and *nodal strength* in the most rostral part of the left middle frontal gyrus (MFG; the node labeled *Frontal_Mid_Orb* in the AAL—Tzourio-Mazoyer et al., 2002, see Figure 7(b)—describes an anatomical region in the orbital part of the left middle frontal gyrus (MFG)—Rolls et al., 2015) was high enough to survive the subsequent correction of 108 (36 nodes, 3 brain states) simultaneous comparisons by applying the false discovery rate correction (Spearman's $r = -.86$).

Figure 4. Continued
and blue rectangles highlight negative correlations or decoupling between the networks/ICs. Further, positive correlations between networks/ICs and subsystems are coded in warm/red colors, and negative correlations between networks/ICs and subsystems in cold/blue colors.

SWA = sliding windows analysis; IC = independent components; IOG = inferior occipital gyrus; ACC = anterior cingulate; SMA = supplementary motor area; DAN = dorsal attention network; FPN = frontoparietal network; LECN = left executive-control network; RECN = right executive-control network; aDMN = anterior default mode network; pDMN = posterior default mode network; MTG = middle temporal gyrus.
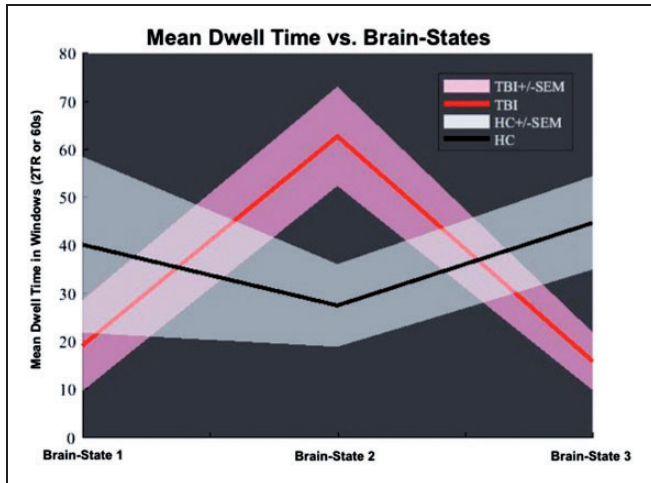
Figure 5. Mean dwell time versus brain states. Illustration of the group-specific differences in dwell time. While the healthy controls spent about the same time in each of the brain states, the concussion group spent most of the time during the resting-state scan in Brain State 2 and clearly less time in the Brain States 1 and 3. The *t* test revealed groupwise significant differences between the dwell times for Brain States 2 and 3. The concussion group spent significantly more time in Brain State 2 ($t = 2.62$; $p = .0254$) than the healthy controls, and the latter spent significantly more time in Brain State 3 ($t = 2.532$; $p = .0302$) than the concussion group. TBI = traumatic brain injury; HC = healthy control; SEM = standard error of the mean.

Discussion

In this present pilot study, we set out to investigate the consequences and implications of hyperconnectivity in fMRI resting-state networks and to determine how the injury-related structural changes are associated with the functional phenomenon of hyperconnectivity in a group of adolescents with concussion.

For this purpose, we reanalyzed a subsample of a data set from our previous studies that showed hyperconnectivity in adolescents diagnosed with concussion (Borich et al., 2015) as well as diffuse axonal injuries (Virji-Babul et al., 2013) and formulated two hypotheses: (a) Hyperconnectivity or the prolonged synchronization of parts of the intrinsic network architecture will be evident as a disruption of the highly dynamical interplay between the different ICNs in the adolescents diagnosed with concussion compared with network dynamics of the healthy controls, and (b) the structural integrity of brain regions belonging to the so-called rich club will be associated with the disrupted intrinsic brain dynamic in adolescents with concussion.

By using a SWA to model three common brain states or network-configurations for the concussed and the healthy adolescents, we confirm our first hypothesis. We show that concussed adolescents spent the majority of time in Brain State 2 within the context of resting state
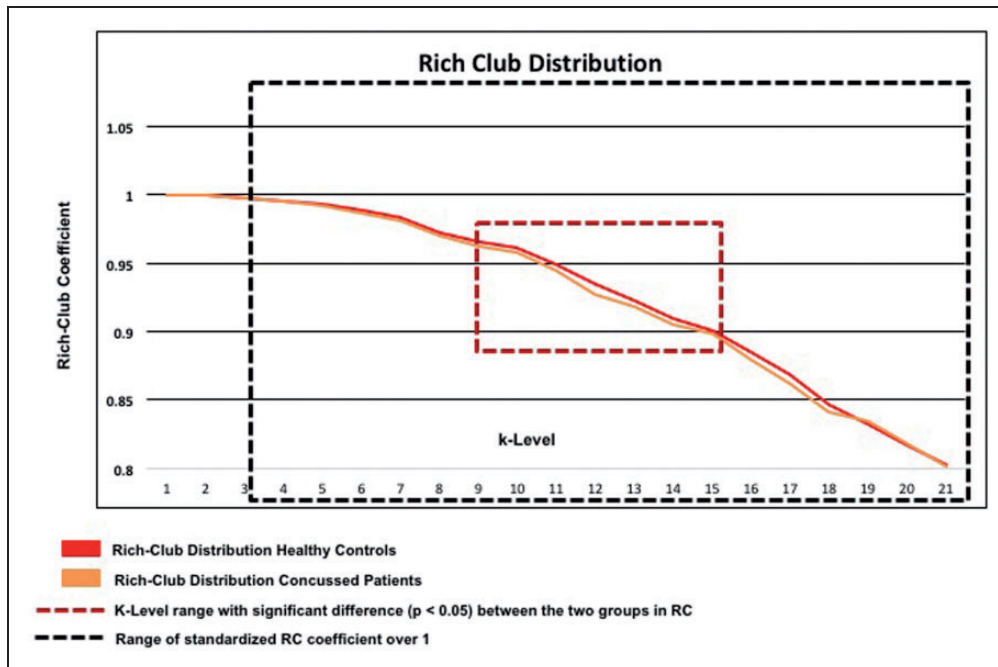

Figure 6. Weighted rich club distribution of the adolescents diagnosed with concussion and the healthy controls. RC = rich club.

Table 3. K-Level Range of Significant Differences in the *Rich Club Distribution* Between Healthy Controls and Patients.

K level	K1	K2	K3	K4	K5	K6	K7	K8	K9	K10	K11	K12	K13	K14	K15
Wilcoxon W	36.0	33.0	38.0	37.0	32.0	32.0	29.0	28.0	23.0	21.0	24.0	27.0	27.000	29.0	26.0
Z	−1.0	−.964	−.160	−.321	−1.123	−1.123	−1.604	−1.764	−2.567	−2.887	−2.406	−1.925	−1.925	−1.604	−2.085
Exact Sig. (one tailed)	.500	.186	.452	.389	.145	.144	.063	**.044***	**.004***	**.001***	**.008***	**.030***	**.030***	.063	**.019***

Note. Table 3 shows the results of the one-sided nonparametric Wilcoxon–Mann test to determine the *k* levels for which the *rich club coefficient* of the healthy controls was significantly higher than the *rich club coefficient* of the patients. The bold letters indicate the *k* levels of the rich club distribution for which we found significant differences between healthy and adolescents with concussion.
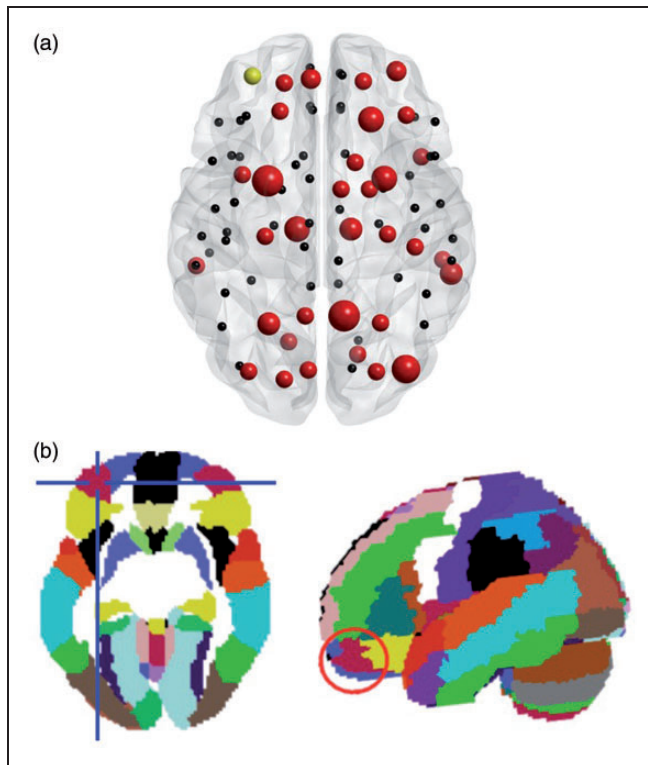

Figure 7. Illustration of the rich club members in the healthy controls. (a) Localization of the analyzed rich club nodes in the healthy controls. The red color indicates a rich club node, the size of the red nodes relates to their degree. Yellow marks the node in the most rostral part of left middle frontal gyrus whose value in nodal strength value was significantly associated (Spearman's $r = -.86$) with the subjects' dwell time in Brain State 3. (b) Localization (regions highlighted by red circle) of the node in the AAL template.

and therefore seemed to be quasi *stuck* in this brain state. In contrast, healthy adolescents switched dynamically and smoothly between three brain states and spend approximately the same time in each state. In addition, while the adolescents with concussion spent significantly more time in Brain State 2 than the healthy adolescents, the latter spend significantly more time in Brain State 3 than the concussed group.

We also confirm our second hypothesis by using GTA (nodal strength, betweenness centrality), DTI, and FA as the diffusion characteristics describing the integrity of the structural brain connectivity to model the rich club members. We found that the nodal strength of a rich club node in the most rostral part of the left MFG was negatively associated with the length of time or dwell time that the adolescents spent in Brain State 3. As the SWA had previously revealed that the adolescents with concussion spent significantly less time than their healthy counterparts in Brain State 3, we interpret this finding to mean that the higher nodal strength in this left frontal region is associated with less time spent in Brain State 3, and this may be related to the persistent, injury-related axonal changes. These axonal changes may inhibit the smooth and dynamic transition from one brain state to another. In particular, switching from Brain State 2 to brain state 3 seems to be more affected by the consequences of type of injury.

While our pilot study is the first study to focus on how concussion-related hyperconnectivity affects the dynamics of the intrinsic activity of the brain in adolescents, two other studies have investigated this relationship in adults with TBI that are important to mention. Mayer et al. (2015) used the same analysis methods, that is, a stationary ICA to model the ICNs followed by a SWA, and the same software, the Group ICA of fMRI Toolbox (GIFT; http://mialab.mrn.org/software/gift/). However, there are important differences between the two studies. Our study sample was highly homogeneous (i.e., very small age range, similar socioeconomic background and educational level, same physical activity level, and the injured adolescents had sustained a concussion while playing ice hockey). The study sample reported by Mayer et al. (2015) was well powered with 48 patients and 48 healthy controls; however, the concussed patients were recruited from local emergency departments and had a much more heterogeneous demographic. In addition, the two studies differ in the time between injury and MRI data acquisition. The cohort in the Mayer et al. (2015) study

Table 4. Identification of the Rich Club Nodes in the Healthy Controls.

Node	Degree	<0.05 uncorr.	Node	Degree	<0.05 uncorr.
Precuneus L	59	BS2-NS	Frontal Sup L	38	
Putamen L	57		Hippocampus R	38	
Occipital Mid L	48	BS3-BC	Occipital Sup L	38	
Thalamus L	48	BS3-NS BS3-BC	Temporal Inf R	38	BS1-BC
Frontal Sup R	47		Frontal Inf Orb L	37	BS2-NS
Putamen R	47		Frontal Inf Orb L	37	BS2-BC BS3-BC
Thalamus R	47		Caudate R	37	BS2-BC
Parietal Sup L	45		Frontal Sup Orb L	36	
Precuneus R	45		Frontal Mid R	36	
Temporal Mid R	44	BS1-BC	Frontal Mid Orb L	36	BS3-NS*** BS3-BC
Occipital Mid R	44		Cuneus L	36	
Frontal Mid Orb R	43		Occipital Sup R	36	BS2-BC
Frontal Sup Medial L	42	BS3-NS BS3-BC	Occipital Inf R	36	BS2-NS BS2-BC
Temporal Mid L	42		Postcentral R	36	
Frontal Sup Orb R	41		Temporal Pole Mid R	36	
Insula L Lingual L	40		Hippocampus L	35	
Lingual L	40		Calcarine R	35	
Parietal Sup R	40		Pallidum R	35	BS2-NS

Note. List of the 36 rich club nodes in the structural brain architecture of the healthy adolescents arranged in descending order of their degree value. BS = brain state; NS = nodal strength; BC = betweenness centrality. The three asterisks *** indicate the only node that showed a negative significant association of nodal strength and dwell time in Brain State 3 after false discovery rate correction for multiple comparisons.

underwent the MRI examination in the first 21 days after the injury (average time between injury and MRI = 14 days), while the MRI data of our adolescents were acquired on average, 27 days after injury. Furthermore, Mayer et al. (2015) proposed an a priori hypothesis, expecting to find altered intrinsic dynamics in the DMN and the subcortical regions of the brain in the concussed group. They also used different outcome measurements, as they computed the standard deviation across the sliding windows correlation time series as a summary of temporal variability, and following this rationale, a high standard variation was interpreted as an indicator of a variable or more less stable functional connections between two ICNs (Mayer et al., 2015). To quantify the intrinsic brain dynamics in a global and spatially invariant way with a single parameter, the authors used an additional measurement, the so-called DisCo-Z (Mayer et al., 2015). They found reduced connectivity in the static connectivity in the DMN in the TBIs before false discovery rate correction and a trend for decreased dynamic connectivity in patients across all ICNs measured by the DisCo-Z. After correcting for multiple comparisons, the authors did not find evidence for significant group differences in the static connectivity measurement nor in the computed dynamic parameters. Due to these differences, the findings of our pilot study and those of Mayer et al. (2015) cannot easily be compared.

Hellyer et al. (2015) conducted a study to evaluate the importance of intrinsic metastability as an operating principle of the brain. The term *metastability* describes a specific modus operandi of the brain in which neural ensembles are able to coordinate rapidly, flexibly engaging and disengaging without becoming locked into fixed interactions (Hellyer et al., 2015). Metastability at rest was found to be higher than during a focused cognitive task (Hellyer et al., 2014). High metastability during rest is thought to represent a state of the brain with large variability in functional configuration. Therefore, high metastability may be unfavorable during goal-driven behavior and cognitive tasks as these require a specific and stable configuration of task-related brain networks (Hellyer et al., 2014). The condition after a TBI was chosen by the authors in particular because it represents a preeminent example of white matter disconnection disorder producing characteristic cognitive impairments by affecting processing speed and cognitive flexibility (Hellyer et al., 2015). For this purpose, the authors analyzed the resting-state fMRI and DTI data of 63 patients (*M* age 37.4 years, the majority of the patient sample was diagnosed with moderate to severe TBI) in the chronic phase of TBI (on average 5.48 months after injury) and 27 controls. They found that the TBI group was characterized by low general metastability and a widespread reduction in FA across the white matter skeleton.

Further, the global metastability was significantly associated with the white matter integrity only in the TBI group. This was particularly evident in the integrity of the white matter tracts connecting the frontal cortex with the thalamus (Hellyer et al., 2015). In combination with the cognitive and behavioral results, Hellyer et al. interpreted the general low metastability in the TBI group as an indicator that their brain needs more time and is less reliable when changing between different cognitive states and has a generally smaller repertoire of brain states to facilitate cognitive processes. In spite of the different methodological approaches and etiology of brain injury, the main findings across these studies are similar: Individuals across the spectrum from mild to severe TBI show impaired temporal dynamics that is reflected as impaired switching from one brain configuration to another.

How this impairment or delayed switching impacts cognition and behavior is still unclear. Because we have no detailed neuropsychological data of our study sample, we can only cautiously speculate based on the cognitive and behavioral problems that are frequently reported in the literature. We do this cautiously as we are well aware that our adolescent cohort is undergoing a rapid phase of brain development, especially in the white matter architecture, and findings from this age-group cannot easily be generalized to other age-groups.

We found that the adolescents with concussion of our study sample spent significantly more time in a brain state whose network configuration pattern is characterized by decoupling or segregation of the three subsystems, that is, the visual, motor, and auditory network forming the *primary-perception-production* subsystem, the attentional networks grouping together as an in-output-attention interface and networks representing the higher order cognitive subsystem. In contrast, the healthy controls spent significantly more time in a brain state where the primary-perception-production subsystem and the attentional subsystem showed a high positive coupling or integration. Guided by these distinct differences of the two brain states, we discuss the potential behavioral and cognitive consequences of our findings.

Attention is a highly complex function that can be divided into different cognitive operations that are themselves quite complex. Attention has to be allocated and the focus of attention has to be maintained during the task at hand and irrelevant external distractions must be disregarded. Simultaneously, the brain has to be able to disengage efficiently and quickly to reallocate its attentional focus as soon as it detects an unexpected or salient external event to which it needs to react in a behaviorally adaptive way (Corbetta et al., 2000; Corbetta and Shulman, 2002). All these different cognitive suboperations are accomplished in the brain by a timely and fine-tuned interplay of different attention networks with the visual and auditory networks as input-processing systems and the motor network as a (re)acting system (Corbetta et al., 2000; Corbetta and Shulman, 2002).

Our findings suggest that the intrinsic functional architecture of adolescents with concussion appears to be stuck in a network configuration that is quite distant from the network configuration needed for attentional processes. Specifically, these dynamics seem to gravitate toward a configuration that is characterized by an inherent functional segregation of the functional networks that are required for attention. The necessary reconfiguration to meet the demands of these attention operations as well as the stable maintenance of this configuration over the time are likely to be more time-consuming, energetically costlier and more exhaustive for a brain recovering from concussion than for a healthy brain.

We cautiously interpret our findings in light of findings that show that transient cognitive problems in the domains of executive-control, long-term memory, working memory, and processing speed in individuals with concussion (Toledo et al., 2012; Howell et al., 2013; Mayr et al., 2014; Barker-Collo et al., 2015). Each of these cognitive functions contains an attentional component, that is, either requiring focused concentration for a prolonged period of time or the ability to quickly disengage and reorient to a new stimulus.

The inability of the adolescents with concussion to switch as quickly and smoothly as their healthy peers into a more suitable network-configuration for attentional processes seems to be associated with an injury-caused white matter abnormality of a region underlying the most rostral part of the left middle frontal gyrus (MFG). Our structural graph theoretical analyses revealed that the nodal strength of this region was significantly negatively associated with the dwell time in Brain State 3. Nodal strength is a graph analysis metric that not only takes in account the number of connections of a region but also weights the connections by their strength. A high value in nodal strength can be caused either by the number of connections, or by the strength of these connections, or by the combination of both elements. We used FA to model the strength of a connection. FA quantifies the degree of directionality of diffusion of water in the brain tissues. While water molecules can freely diffuse in all directions in the cerebrospinal fluid and almost unconstrained in the gray matter, that is, the diffusion is isotropic, the white matter axons constrain the freedom of the directionality of diffusion. The main diffusion direction in healthy, well-organized and fully myelinated white matter is along the axons, that is, the diffusion is practically one-directional or anisotropic (Niogi and Mukherjee, 2010).

Although a high FA value is commonly interpreted as indicator of white matter integrity and therefore an

appropriate feature to describe connection strength, abnormally elevated FA values, that is, higher FA values than in the healthy controls in particular, are typically found in individuals with concussion during the acute and subacute periods (Niogi and Mukherjee, 2010; Eierud et al., 2014). These elevated values are interpreted as the consequence of trauma-related axonal swelling that transiently restricts the interstitial space, which results in an increase in anisotropic diffusion and in higher FA values in the regions of axonal swelling (Niogi and Mukherjee, 2010). In line with this, we interpreted the higher nodal strength value found in the white matter underlying the most rostral part of the left middle frontal gyrus in the adolescents with concussion as caused by the higher FA values in this region and as an indicator of injury-related persistent axonal swelling.

Furthermore, we were able to identify this region as a rich club member and by virtue of this membership as a highly influential hub as well as a constituent region of the structural backbone of the brain in our adolescent study sample. It is still an open question how the coherent and dynamically changing spatiotemporal patterns of slow frequent (<0.1 Hz) spontaneous fluctuations of the BOLD-signal, which we measure when we acquire resting-state fMRI data, emerge from by the underlying white matter architecture (Park and Friston, 2013). While the underlying white matter tracts certainly constrain the functional repertoire of this intrinsic activity and a direct structural connection predicts a functional connection (Hagmann et al., 2008; Deco et al., 2016; Betzel et al., 2016), the opposite conclusion cannot be drawn. An existing structural connection is not at all necessary for the emergence of intrinsic connectivity between two regions of the same network (Betzel et al., 2016; Mišić et al., 2016) and even less for the existence of temporal and spatial dynamical interactions between networks or single network regions (de Pasquale et al., 2012; Karahanoğlu and Van de Ville, 2015; Betzel et al., 2016; Mišić et al., 2016). Studies investigating the question how the intrinsic dynamics of the brain are related to the underlying anatomical network (Gollo et al., 2015; Betzel et al., 2016; Deco et al., 2016; Mišić et al., 2016) agree that the white matter configuration of densely interconnected brain regions, which was dubbed rich club because of the constituent regions' tendency to mainly connect among peers, that is, among similar highly influential hub nodes than themselves (van den Heuvel and Sporns, 2011), is particularly important. These studies seem to corroborate our argument that an injury-related structural impairment in only a single brain region can reasonably be associated with the slowed-down dynamics of several different resting-state networks that we established as a characteristic functional feature in the brains of the concussed group.

Limitations

The study presented here is a pilot study and was motivated by our interest to gain a better understanding of what hyperconnectivity means in concussion. Because the research question of the former projects differed from our current research interest, we did not have the neuropsychological data necessary to directly relate our functional and structural findings to the behavioral and cognitive problems of our concussed group but had to associate them to behavioral findings reported in the literature.

In addition, resting-state data are notoriously noisy, and the results of resting-state analyses are highly sensitive to motion artifacts. This problem is exacerbated when dynamical analysis methods are used as we did. As a consequence of our efforts to minimize all possible corrupting confounds caused by motion artifacts as rigorously as possible, we had to exclude 10 participants of the original data set and ended up with only 6 participants in each group.

One advantage of this small sample size is that we have a highly homogeneous sample that was further matched for all possible residual motion confounds that may have survived our rigorous efforts to reduce them. Because of this, we are confident that that our findings are directly linked to the consequences of a concussion and not due to other factors.

Conclusion

The consequences of concussion are still not very well understood. We used a combination of recently developed analysis methods—dynamical resting-state analysis and GTA—to better understand the changes in brain structure and functions following a concussion and how these changes relate to each other.

Our preliminary results reveal that concussion results in specific changes in network dynamics that are characterized by a lack of flexibility in shifting between two brain states of which one is characterized by a clear segregation of the primary-perception-production subsystem from the attentional subsystem and the other by a clear integration of the primary-perception-production subsystem from the attentional subsystem. We suggest that the lack of dynamic flexibility in the concussed group may be due an increased nodal strength of a rich club node in the most rostral part of the left MFG. We interpret the increased nodal strength of this frontal region as an indicator of changes in the axonal structure of the underlying white matter structure, the left corona radiata, and cautiously speculate that our findings may explain why adolescents with concussion have difficulties with tasks that require focused attention over a long time period or switching the attentional focus when salient or unexpected new external stimuli require a reallocation of attention. Longitudinal studies with a larger sample

combined with specific cognitive measures will provide further insights into the nature of these changes following concussion.

Summary Statement

Adolescents with concussion show significant changes in brain dynamics in the resting state characterized by a lack of dynamic flexibility and associated changes in network structure. These alterations in network organization may reflect attention deficits typically reported following concussion.

Declaration of Conflicting Interests

Funding

References

Agarwal, S., Stamatakis, E. A., Geva, S., & Warburton, E. A. (2016). Dominant hemisphere functional networks compensate for structural connectivity loss to preserve phonological retrieval with aging. *Brain Behav*, *6*(9): e00495.

Anderson, V., Spencer-Smith, M., Leventer, R., Coleman, L., Anderson, P., Williams, J., Greenham, M., & Jacobs, R. (2009). Childhood brain insult: Can age at insult help us predict outcome? *Brain A J Neurol*, *132*, 45–56.

Ashburner, J. (2007). A fast diffeomorphic image registration algorithm. *Neuroimage*, *38*, 95–113.

Barker-Collo, S., Jones, K., Theadom, A., Sarkey, N., Dowell, A., McPherson, K., Ameratunga, S., Dudley, M., Te Ao, B., & Feigin, V. (2015). Neuropsychological outcome and its correlates in the first year after adult mild traumatic brain injury: A population-based New Zealand study. *Brain Inj*, *29*(13–14): 1604–1616.

Barlow, K. M., Crawford, S., Stevenson, A., Sandhu, S. S., Belanger, F., & Dewey, D. (2010). Epidemioogy of postconcussion syndrome in pediatric mild traumatic brain injury. *Pediatrics*, *126*, e374–e381.

Betzel, R. F., Gu, S., Medaglia, J. D., Pasqualetti, F., & Bassett, D. S. (2016). Optimally controlling the human connectome: The role of network topology. *Sci Rep*, *6*, 30770.

Bharat, R. D., Munivenkatappa, A., Gohei, S., Panda, R., Saini, J., Rajeswaran, J., Shukla, D., Bhagavatula, I. D., & Biswal, B. B. (2015). Recovery of resting brain connectivity ensuing mild traumatic brain injury. *Front Hum Neurosci*. Advance online publication. doi:10.3389/fnhum.2015.00513.

Bonelle, V., Ham, T. E., Leech, R., Kinnunen, K. M., Mehta, M. A., Greenwod, R. J., & Sharp, D. (2012). Salience network integrity predicts default mode network function after traumatic brain injury. *Proc Natl Acad Sci U S A*, *109*(20): 4690–4695.

Bonelle, V., Leech, R., Kinnunen, K. M., Ham, T. E., Beckmann, C. F., De Boissezon, X., Greenwood, R. J., & Sharp, D. J. (2011). Default mode network connectivity predicts sustained attention deficits after traumatic injury. *J Neurosci*, *31*(38): 13442–13452.

Borich, M., Babul, A. N., Yuan, P. H., Boyd, L., & Virji-Babul, N. (2015). Alterations in resting-state brain networks in concussed adolescent athletes. *J Neurotrauma*, *32*(4): 265–271.

Borich, M., Makan, N., Boyd, L., & Virji-Babul, N. (2013). Combining whole-brain voxel-wise analysis with in-vivo tractography of diffusion behavior after sports-related concussion in adolescents: A preliminary report. *J Neurotrauma*, *30*(14): 1243–1249.

Burianová, H., Marstaller, L., Choupen, J., Sepehrband, F., Zisei, M., & Reutens, D. (2015). The reation of structural integrity and task-related functional connectivity in the aging brain. *Neurobiol Aging*, *36*(10): 2830–2838.

Caeyenberghs, K., Leemans, A., Leunissen, I., Gooijers, J., Michels, K., Sunaert, S., & Swinnen, S. P. (2014). Altered networks and executive deficits in traumatic brain injury patients. *Brain Struct Funct*, *19*(1): 193–209.

Caeyenberghs, K., Verhelst, H., Clemente, A., & Wilson, P. (2017). Mapping the functional connectome in traumatic brain injury: What can graph metrics tell us? *Neuroimage*, *160*, 113–123.

Calhoun, V. D., Adali, T., Pearlson, G. D., & Pekar, J. J. (2001). A method for making group inferences from functional MRI data using independent component analysis. *Hum Brain Mapp*, *14*, 140–151.

Chang, C., & Glover, G. H. (2010). Time-frequency dynamics of resting-state brain connectivity measured with fMRI. *Neuroimage*, *50*, 81–98.

Chang, L. C, Jones, D. K., & Pierpaoli, C. (2005). RESTORE: Robust estimation of tenors by outlier rejection. *Magn Reson Med*, *53*(5): 1088–1095.

Churchill, N. W., Hutchison, M. G., Richards, D., Leung, G., Graham, S. J., & Schweizer, T. A. (2017). The first week after concussion: Bood flow, brain function and white matter microstructure. *Neuroimage Clin*, *14*, 480–489.

Cole, D. M., Smith, S. M., & Beckmann, C. (2010). Advances and pitfalls in the analysis and interpretation of resting-state FMRI data. *Front Syst Neurosci*, *4*, article 8.

Corbetta, M., Kincade, J. M., Ollinger, J. M., McAvoy, M. P., & Shulman, G. L. (2000). Voluntary orienting is dissociated from target detection in human posterior parietal cortex. *Nat Neurosci*, *3*(3): 292–297.

Corbetta, M., & Shulman, G. L. (2002). Control of goal directed and stimulus driven attention in the brain. *Nat Rev Neurosci*, *3*(3): 201–215.

Czerniak, S. M., Sikoglu, E. M., Liso Navarro, A. A., McCarthy, J., Eisenstock, J., Stevenson, J. H., King, J. A., & Moore, C. M. (2015). A resting state functional magnetic resonance imaging study of concussion in collegiate athletes. *Brain Imaging Behav*, *9*(2): 323–332.

Deco, G., Van Hartevelt, T. J., Fernandes, H. M., Stevner, A., & Kringelbach, M. L. (2016). The most relevant human brain regions for functional connectivity: Evidence for a dynamical workspace of binding nodes from whole-brain computational modeling. *Neuroimage*, *146*, 197–210.

De Pasquale, F., Della Penna, S., Snyder, A. Z., Marzetti, L., Pizzella, V., Romani, G. L., & Corbetta, M. (2012). A cortical core for dynamic integration of functional networks in the resting human brain. *Neuron*, *74*, 753–764.

Eierud, C., Craddock, R. C., Fletcher, S., Aulakh, M., King-Casas, B., Kuehl, D., & LaConte, S. M. (2014). Neuroimaging after mild traumatic brain injury: Review and meta-analysis. *Neuroimage Clin*, *4*, 283–294.

Gardner, R. J., & Yaffe, K. (2015). Epidemiology of mild traumatic brain injury and neurodegenerative disease. *Mol Cell Neurosci*, *66*, 75–80.

Gollo, L. L., Zalesky, A., Hutchison, R. M., van den Heuvel, M., & Breakspear, M. (2015). Dwelling quietly in the rich club: Brain network determinants of slow cortical fluctuations. *Philos Trans R Soc Lond B Biol Sci*, *370*(1668): pii: 20140165.

Hagmann, P., Cammoun, L., Gigandet, X., Meuli, R., Honey, C. J., Wedeen, V. J., & Sporns, O. (2008). Mapping the structural core of human cerebral cortex. *Plos Biol*, *6*(7): e 159. doi:10.1371/journal.pbio.0060159.

Harris, N. G., Verley, D. R., Gutman, B. A., Thompson, P. M., Yeh, H. J., & Brown, J. A. (2016). Disconnection and hyper-connectivity underie reorganization after TBI: A rodent functional connectomic analysis. *Exp Neurol*, *277*, 124–136.

Hayes, J. P., Logue, M. W., Sadeh, N., Spielberg, J. M., Verfaellie, M., Hayes, S. M., Reagan, A., Salat, D. H., Wolf, E. J., McGlinchey, R. E., Milberg, W. P., Stone, A., Schichman, S. A., & Miller, M. W. (2017). Mild traumatic injury is associated with reduced cortical thickness in those at risk for Alzheimer's disease. *Brain*, *140*(3): 813–825.

Hellyer, P. J., Leech, R., Ham, T. E., Bonelle, V., & Sharp, D. J. (2013). Individual prediction of white matter injury following traumatic brain injury. *Ann Neurol*, *73*(4): 489–499.

Hellyer, P. J., Scott, G., Shanahan, M., Sharp, D. J., & Leech, R. (2015). Cognitive flexibility through metastable neural dynamics is disrupted by damage to the structural connectome. *The J Neurosci*, *35*(24): 9050–9063.

Hellyer, P. J., Shanahan, M., Scott, R., Wise, R. J. S., Sharp, D. J., & Leech, R. (2014). The contro of global brain dynamics: Opposing actions of fronto-parietal control and default mode networks on attention. *The J Neurosci*, *34*(2): 451–461.

Hillary, F. G., Rajtmajer, S. M., Roman, C. A., Medaglia, J. D., Slocomb-Diuzen, J. E., Calhoun, V. D., Good, D. C., & Wylie, G. R. (2014). The rich get richer: Brain injury elicits hyperconnectivity in core subnetworks. *Plos One*, *9*(8): e104021.

Himberg, J., Hyvärinen, A., & Esposito, F. (2004). Validating the independent components of neuroimaging time-series via clustering and visualization. *NeuroImage*, *22*(3): 1214–1222.

Howell, D., Ostering, L., Van Donkelaar, P., Mayr, U., & Chou, L. S. (2013). Effects of concussion on attention and executive function in adolescents. *Med Sci Sports Exerc*, *45*(6): 1030–1037.

Hutchison, M. R., Womelsdorf, T., Allen, E. A., Bandettini, P. A., Calhoun, V. D., Corbetta, M., Della Penna, S., Duyn, J. H., Glover, G. H., Gonzalez-Castillo, J., Handwerker, D. A., Keilholz, S., Kiviniemi, V., Leopold, D. A., de Pasquale, F., Sporns, O., Walter, M., & Chang, C. (2013). Dynamic functional connectivity: Promise, issues, & interpretations. *Neuroimage*, *80*, 360–378.

Iraji, A., Chen, H., Wiseman, N., Welch, R. D., O'Neill, B. J., Haacke, E. M., Liu, T., & Kou, Z. (2016). Compensation through functional hyperconnectivity: A longitudinal connectome assessment of mild traumatic brain injury. *Neural Plast*, *2016*, 4072402. doi:10.1155/2016/4072402.

Johnson, B., Zhang, K., Gay, M., Horovitz, M., Hallett, M., Sebastianelli, W., & Slobounov, S. (2012). Alteration of brain default network in subacute phase of injury in concussed individuals: Resting-state fMRI study. *Neuroimage*, *59*, 511–518.

Jones, D. T., Prashanti, V., Murphy, M. C., Gunter, J. L., Senjem, L. M., Machulda, M. M., Przybelski, S. A., Gregg, B. E., Kantarci, K., Knopman, D. S., Boeve, B. F., Petersen, R. C., & Jack, C. R. Jr. (2012). Non-stationarity in the "resting brain's" modular architecture. *Plos One*, *7*(6): e39731.

Karahanoğlu, F. I., & Van De Ville, D. (2015). Transient brain activity disentangles fMRI resting-state dynamics in terms of spatially and temporally overlapping networks. *Nature Communications*, *6*, 7751–7760.

Laumann, T. O., Snyder, A. Z., Mitra, A., Gordon, E. M., Gratton, C., Adeyemo, B., Gilmore, A. W., Nelson, S. M., Berg, J. J., Greene, D. J., McCarthy, J. E., Tagliazucchi, E., Laufs, H., Schlaggar, B. L., Dosenbach, N. U. F., & Petersen, S. E. (2017). On the stability of BOLD fMRI correlations. *Cereb Cortex*, *27*(10): 4719–4732.

Leemans, A., Jeurissen, B., Sijbers, J., & Jones, D. K. (2009). "ExploreDTI: A graphical toolbox for processing, analyzing, and visualizing diffusion MR data". Paper presented at the Proceedings of the 17th Scientific Meeting, International Society for Magnetic Resonance in Medicine, Honolulu, USA (p. 3537).

Leemans, A., & Jones, D. K. (2009). The B-matrix must be rotated when correcting for subject motion in DTI data. *Magn Reson Med*, *61*(6): 1336–1349.

Marstaller, L., Williams, M., Rich, A., Savage, G., & Burianová, H. (2015). Aging and large-scale functional networks: White matter integrity, gray matter volume, and functional connectivity in resting state. *Neuroscience*, *290*, 369–378.

Mayer, A. R., Ling, J. M., Allen, E. A., Klimaj, S. D., Yeo, R. A., & Hanon, F. M. (2015). Static and dynamic intrinsic connectivity following mild traumatic brain injury. *J Neurotrauma*, *32*(14): 1046–1055.

Mayer, A. R., Mannell, M. V., Ling, J., Elgie, R., Gasparovic, C., Phillips, J. P., Doezema, D., & Yeo, R. A. (2009). Auditory orienting and inhibition of return in mild traumatic brain injury: A fMRI study. *Hum Brain Mapp*, *30*(12): 4152–4166.

Mayer, A. R., Mannell, M. V., Ling, J., Gasparovic, C., & Yeo, R. A. (2011). Functional connectivity in mild traumatic brain injury. *Hum Brain Mapp*, *32*(11): 1825–1835.

Mayr, U., Kuhns, D., & Hubbard, J. (2014). Long-term memory and the control of attentional control. *Cogn Psychol*, *72*, 1–26.

Militana, A. R., Donahue, M. J., Sills, A. K., Solomon, G. S., Gregory, A. J., Strother, M. K., & Morgan, V. L. (2016). Alterations in default-mode network connectivity may be influenced by cerebrovascular changes within a week of sports related concussion in college varsity athletes: A pilot study. *Brain Imaging Behav*, *10*(2): 559–568.

Mišić, B., Betzel, R. F., de Reus, M. A., van der Heuvel, M. P., Berman, M. G., McIntosh, A. R., & Sporns, O. (2016). Network-level structure-function relationship in human neocortex. *Cereb Cortex*, *26*(6): 3285–3296.

Newsome, M. R., Li, X., Wilde, E. A., Ott, S., Biekman, B., Hunter, J. V., Dash, P. K., Taylor, B. A., & Levin, H. B. (2016). Functional connectivity is altered in concussed adolescents athletes despite medical clearance to return to play: A preliminary

report. *Front Neurosci*. Advance online publication. doi:10.3389/fneur.2016.00116.

Niogi, S. N., & Mukherjee, P. (2010). Diffusion tensor imaging of mild traumatic brain injury. *J Head Trauma Rehabil*, *25*(4): 241–255.

Olsen, A., Brunner, J. F., Indredavik Evensen, K. A., Finnanger, T. G., Vik, A., Skandsen, T., Landrø, N. I., & Håberg, A. K. (2015). Altered cognitive control activations after moderate-to-severe traumatic brain injury and their relationship to injury severity and everyday-life function. *Cereb Cortex*, *25*(8): 2170–2180.

Park, H. J., & Friston, K. (2013). Structural and functional brain networks: From connections to cognition. *Science*, *342*, 12384111–12384118.

Power, J. D., Barnes, K. A., Snyder, A. Z., Schlaggar, B. L., & Petersen, S. E. (2012). Spurious but systematic correlations in functional connectivity MRI networks arise from subject motion. *Neuroimage*, *59*(3): 2231–2240.

Rolls, E. T., Joliot, M., & Tzourio-Mazoyer, N. (2015). Implementation of a new parcellation of the orbitofrontal cortex in the automated anatomical labeling atlas. *Neuroimage*, *122*, 1–5.

Rousseeuw, P. J. (1987). Silhouettes: A graphical aid to the interpretation and validation of cluster analysis. *Comput Appl Math*, *20*, 53–65.

Rubinov, M., & Sporns, O. (2010). Complex network measures of brain connectivity: Uses and interpretations. *Neuroimage*, *52*, 1059–1069.

Rubinov, M., & Sporns, O. (2011). Weight-conserving characterization of complex functional brain networks. *Neuroimage*, *56*, 2068–2079.

Sharp, D. J., Scott, G., & Leech, R. (2014). Network dysfunction after traumatic brain injury. *Nat Rev Neurol*, *10*(3): 156–166.

Shumskaya, E., Andriessen, T. M., Norris, D. G., & Vos, P. E. (2012). Abnormal whole-brain functional networks in homogeneous acute mild traumatic brain injury. *Neurology*, *79*(2): 175–182.

Sours, C., George, E. O., Zhou, J., Roys, S., & Gullapalli, R. P. (2015). Hyper-connectivity of the thalamus during the early stages following mild traumatic brain injury. *Brain Imaging Behav*, *983*, 550–563.

Sours, C., Zhou, J., Janowich, J., Arabi, B., Shanmuganathan, K., & Gulapalli, R. P. (2013). Default mode network interference in mild traumatic brain injury – A pilot study. *Brain Res*, *6*(1537): 201–215.

Toledo, E., Lebel, A., Becerra, L., Minster, A., Linman, C., Maleki, N., Dodick, D. W., & Borsook, D. (2012). The young brain and concussion: Imaging as a biomarker for diagnosis and prognosis. *Neurosci Biobehav Rev*, *36*(6): 1510–1531.

Tzourio-Mazoyer, N., Landeau, B., Papathanassiou, D., Crivello, F., Etard, O., Delcroix, N., Mazoyer, B, & Joliot, M. (2002). Automated anatomical labelling of activations in spm using a macroscopic anatomical parcellation of the MNI MRI single subject brain. *Neuroimage*, *15*(1): 273–228.

Van den Heuvel, M. P., & Sporns, O. (2011). Rich club organization of the human connectome. *J Neurosci*, *31*(44): 15775–15786.

Virji-Babul, N., Borich, M. R., Makan, T., Frew, K., Emery, C. A., & Boyd, L. A. (2013). Diffusion tensor imaging of sports-reated concussion in adolescents. *Pediatr Neurol*, *48*(1): 24–29.